Autotrophic Nitrogen Removal in Membrane-Aerated Biofilms: Archaeal Ammonia Oxidation versus Bacterial Ammonia Oxidation

Yiwen Liu[1], Huu Hao Ngo[1], Wenshan Guo[1], Lai Peng[2], Yuting Pan[3], Jianhua Guo[4], Xueming Chen[4], Bing-Jie Ni[4,5,*]

[1] Centre for Technology in Water and Wastewater, School of Civil and Environmental Engineering, University of Technology Sydney, Sydney, NSW 2007, Australia

[2] Laboratory of Microbial Ecology and Technology (LabMET), Ghent University, Coupure Links 653, 9000 Ghent, Belgium

[3] Department of Environmental Science and Engineering, School of Architecture and Environment, Sichuan University, Chengdu, Sichuan 610065, China

[4] Advanced Water Management Centre, The University of Queensland, St. Lucia, Brisbane, QLD 4072, Australia

[5] State Key Laboratory of Pollution Control and Resources Reuse, College of Environmental Science and Engineering, Tongji University, Shanghai 200092, PR China

*Corresponding author:

Bing-Jie Ni, Phone: +61 7 33463230; Fax: +61 7 33654726; E-mail: b.ni@uq.edu.au

Abstract

Recent discovery of ammonia-oxidizing archaea (AOA) not only substantially improved our understanding of the global nitrogen cycle, but also provided new possibilities for nitrogen removal from wastewater. In particular, compared to ammonia-oxidizing bacteria (AOB), the high ammonia oxidation under oxygen-limited conditions driven by AOA is potentially more suitable for autotrophic nitrogen removal in a single-stage membrane aerated biofilm reactor (MABR) through coupling with anaerobic ammonia oxidation (Anammox). In this work, mathematical modeling is applied to assess the system performance and associated microbial community structure of an AOA-Anammox MABR under low- (30 mg N L^{-1}) and high-strength (500 mg N L^{-1}) ammonium conditions, with a side-by-side comparison to an AOB-Anammox MABR system under the same conditions. Results demonstrate that both ammonium surface loading (or hydraulic retention time) and oxygen surface loading significantly affect the system performance. In contrast to AOB-Anammox system, the AOA-Anammox MABR shows higher total nitrogen (TN) removal and lower oxygen supply, with much better repression of NOB and substantially wider operating window for high-level TN removal (>80%) in terms of varied oxygen and ammonium loadings. These results provide first insights and useful information for design and operation of this novel AOA-Anammox MABR system in its potential future applications.

Keywords: ammonia-oxidizing archaea; ammonia-oxidizing bacteria; Anammox; membrane aerated biofilm reactor; mathematical modeling

1. Introduction

Nitrogen removal is one of the crucial processes in wastewater treatment. Conventional biological nitrogen removal (BNR) from wastewater consists of nitrification by ammonia-oxidizing bacteria (AOB) and nitrite-oxidizing bacteria (NOB) followed by denitrification, which cannot satisfy the development requirements for the next generation wastewater treatment processes, such as to enhance energy recovery from organics in wastewater and to reduce the energy consumption/carbon footprint for nitrogen removal [1]. Autotrophic nitrogen removal system has been developed in which, under oxygen-limited conditions, AOB convert ammonia to nitrite, which provides electron acceptor to anaerobic ammonia oxidation (Anammox) bacteria to oxidise the remaining ammonia forming nitrogen gas [2-5].

Compared to the conventional nitrification and denitrification process, this autotrophic process has a lower oxygen demand (hence less aeration and energy consumption) and does not require external carbon source [6]. Such autotrophic system has successfully been implemented in full-scale application [7, 8]. Approximately 100 full-scale autotrophic partial nitritation/anammox systems have been installed worldwide for side-stream (75%) and main-stream (25%) ammonium treatment [9], with 88% of these plants being operated as single-stage systems which would reduce the space as well as decrease both the capital and operational costs compared to two-stage reactor configurations. However, it is typically difficult to achieve high levels of nitrogen removal in one-stage autotrophic systems, because a high dissolved oxygen (DO) concentration inhibits the anammox bacteria and induces the proliferation of NOB while a low DO inhibits the activity of AOB [10, 11]. Further, compared to more widely applied autotrophic treatment for high-strength ammonium, the low-strength ammonium treatment (e.g., main-stream condition) is

being explored at an infancy stage and one of the main challenges is the repression of NOB [11, 12].

It has been demonstrated that autotrophic ammonia oxidation is not conducted exclusively by bacteria (i.e., AOB), and ammonia-oxidizing archaea (AOA) are ubiquitous in various natural environments [13-15] and wastewater treatment systems [16-18]. Recent discovery of AOA not only substantially improved our understanding of the global nitrogen cycle, but also provided new possibilities for BNR from wastewater [19, 20]. In contrast to AOB, AOA often thrive at DO levels of ca. 0.1 mg/L and can achieve higher ammonia oxidation under oxygen-limited conditions [21]. AOA are therefore likely a better partner with Anammox than AOB in autotrophic nitrogen removal process. In natural systems such as marine or soil, substantial experiments have proven AOA could provide nitrite and create anoxic microenvironments for anammox bacteria with oxygen consumption [22]. Thus, an autotrophic nitrogen removal process driven by AOA and Anammox could potentially be an attractive alternative to AOB-Anammox system for achieving complete autotrophic nitrogen removal.

Due to the slow growth rates of AOA and Anammox, biomass retention is crucial for high-rate performance. Biofilms can retain microorganisms with very slow growth kinetics, and biomass can be naturally accumulated in the biofilm at different depths. Particularly, the membrane aerated biofilm reactor (MABR) has evolved in recent years [23-25] and been proved to be suitable for one-stage autotrophic nitrogen removal process [26-29]. In such system, oxygen is supplied through a gas-permeable membrane that also serves as biofilm support. The merits of such a system lie in the high and efficient oxygen transfer through the membrane and also in the potential for a more amenable control strategy due to separation of oxygen and ammonium fluxes.

For example, partial nitrification and completely nitrogen removal were successfully achieved in a single MABR, with a max removal rate of 0.77 kg-N/m^3/d and 88.5% total nitrogen (TN) removal efficiency [27].

Mathematical modelling of wastewater treatment processes is of great importance toward a full understanding of the complex system and the optimization of its practical application [30-34]. Although AOA have several characteristics potentially rendering AOA-Anammox more suitable for AOB-Anammox, such new coupling systems have not been explored yet. In this study, we carry out a model-based assessment of the performance of a novel autotrophic nitrogen removal technology based on AOA and Anammox in one-stage MABR, for both low-strength and high-strength ammonium treatment, with a side-by-side comparison to an AOB-Anammox MABR system. The impacts of key operational parameters on removal efficiency such as oxygen surface loading (L_{O2}) and ammonium surface loading were investigated to provide the first insight into the role of AOA in partial nitrification MABR systems, which may help improve the design and operation of such systems for future applications.

2. Material and methods

2.1 Membrane-aerated biofilm reactors

In an MABR reactor, oxygen is supplied through a gas-permeable membrane that also serves as biofilm support (Figure 1). Applying a counter-diffusional concept, oxygen is provided to the base of the biofilm, whereas other substrates, namely ammonium and bicarbonate, are supplied from the bulk liquid phase [35, 36]. The oxygen and ammonium concentration gradients cause stratification of AOA (or AOB) and Anammox in the biofilm (Figure 1). The simulated MABR in this work has a

working volume of 1 m^3 with a completely mixed liquid phase. The bulk volume and biofilm surface area of the reactor are 0.96 m^3 and 235 m^2, respectively, with a surface to volume ratio of 245 m^2 m^{-3}. Gas-permeable membranes used for oxygen supply and biofilm attachment have about 0.04 m^3 gas volume inside the membrane lumen. Compressed air is supplied in flow-through mode to the membrane module, with the oxygen flux to the biofilm controlled through changing either the applied gas pressure or the gas flow rate into the membrane lumen. In this work, the simulated low-strength ammonium concentration is set at 30 mg N L^{-1} representing main-stream condition [12] while high-strength ammonium concentration is 500 mg N L^{-1} mimicking side-stream condition [9]. The influent flow rate is varied to regulate the influent ammonium surface loading, which also corresponds to hydraulic retention time (HRT) in this case.

2.2 Mathematical models

The kinetics and stoichiometry of the biological reaction model for the one-stage autotrophic nitrogen removal system driven by AOA and Anammox (Figure 1A) are summarized in Tables 1 and 2. Both growth and decay processes are considered for each species, i.e., AOA, NOB, Anammox and heterotrophs. Kinetic control of all the microbial reaction rates is described by the Monod equation, with each reaction rate modelled by an explicit function considering all substrates involved. The parameters used regarding the metabolisms of AOA, NOB, Anammox and heterotrophs are listed in Table S1 in the Supporting Information (SI) with the definitions, values and units. For the one-stage autotrophic nitrogen removal system driven by AOB and Anammox (Figure 1B), the kinetics and stoichiometry of the biological reaction model for AOB-Anammox MABR system are well established previously in literature [35-37], and

thus presented in Tables S2-S4 (SI).

The multi-species one-dimensional biofilm model is then constructed to simulate the biotransformation and microbial community structure in the MABR, employing the software AQUASIM 2.1d [38]. The MABR is modelled through integrating a completely mixed gas compartment (representing the membrane lumen operated as flowthrough) with a biofilm compartment, containing the biofilm and bulk liquid. The gas compartment is connected to the base of the biofilm via a diffusive link. The gaseous concentration of oxygen in the gas compartment is determined by the applied gas pressure and the gas flow rate. The oxygen flux from the gas to the biofilm matrix compartment through the membrane is modelled based on Henry law [35, 36]. Biofilm structures are represented as a continuum without considering diffusive mass transport of biomass in the biofilm matrix. The steady-state biofilm thickness is established by controlling the detachment using a global detachment velocity [35]. The water fraction of the biofilm matrix is 0.75, while the biomass density is 50000 g COD m^{-3} [35, 36]. Parameters regarding biofilm density and porosity, as well as the mass transfer coefficients for ammonium, nitrite, nitrate and oxygen are selected according to Hao et al. [39].

2.3 Scenarios for assessment

Eight different scenarios are considered for the comparison between AOA-Anammox and AOB-Anammox MABR systems in this work, as detailed in Table 3. The first two scenarios (Scenarios 1 and 2) assess the mechanisms behind each system for low-strength and high-strength nitrogen removal, respectively, through generating depth profiles of nitrogen species and DO as well as microbial community distribution in the biofilm. The applied oxygen surface loading (L_{O_2}), ammonium

concentration, HRT (corresponding to ammonium surface loading) and biofilm thickness (L_f) are 0.45 g m^{-2} d^{-1}, 30 mg N L^{-1}, 0.5 d and 200 µm for the low-strength treatment, respectively, while 0.95 g m^{-2} d^{-1}, 500 mg N L^{-1}, 5 d and 500 µm for the high-strength treatment, respectively.

Scenarios 3 and 4 examine the effects of L_{O_2} and HRT on the TN removal and microbial community structure for both AOA-Anammox and AOB-Anammox MABR biofilms under low-strength ammonium condition (containing ammonium of 30 mg N L^{-1}) at steady state. The operational parameters for simulation are chosen systematically over wide ranges of L_{O_2} (0.19 – 0.95 g m^{-2} d^{-1}) and HRT (0.25 – 0.75 d) given a flow rate varying from 3.84 to 1.28 m^3 d^{-1}. Scenarios 5 and 6 test the effects of L_{O_2} and HRT on the TN removal and microbial community structure for the two MABR biofilms under high-strength ammonium condition (containing ammonium 500 mg N L^{-1}) at steady state, with the variations of L_{O_2} (0.19 – 1.90 g m^{-2} d^{-1}) and HRT (2 – 10 d) given a flow rate varying from 0.48 to 0.096 m^3 d^{-1}. Scenarios 7 and 8 then assess the combined impact of L_{O_2} and HRT on the process performance in order to compare the optimal operating windows for AOA-Anammox and AOB-Anammox MABRs under different conditions.

For each scenario, the initial concentrations of all soluble components are assumed to be zero in both biofilm and bulk liquid phases. An average biofilm thickness is applied in the model without consideration of its variation with locations. All simulations assume an initial biofilm thickness of 20 µm. Compared to the low-strength MABR, the high-strength MABR usually undergoes a shorter HRT, giving rise to a greater shear force. Therefore, a lower steady-state biofilm thickness is used to simulate the low-strength MABR (i.e., 200 µm) while a higher steady-state biofilm thickness is considered for the high-strength MABR (i.e., 500 µm). Simulations are

typically run for up to 1500 days to reach steady-state conditions in terms of effluent quality, biofilm thickness, and biomass compositions in biofilms. The steady-state TN removal is used to evaluate the performance of MABR.

3. Results

3.1 MABR performances under low- and high-strength conditions

For the low-strength AOA-Anammox MABR operated in Scenario 1 (Table 3), the steady-state effluent NH_4^+, NO_2^- and NO_3^- concentrations are 2.3 mg N L^{-1}, 0 mg N L^{-1}, and 1.8 mg N L^{-1}, respectively, resulting a TN removal efficiency of 86.3%, higher than that of 83.0% in low-strength AOB-Anammox MABR with NH_4^+, NO_2^- and NO_3^- concentrations of 2.6 mg N L^{-1}, 0 mg N L^{-1}, and 2.5 mg N L^{-1} in the effluent, respectively. The steady-state performances of the high-strength AOA-Anammox and AOB-Anammox MABR systems under the operational conditions of Scenario 2 (Table 3) are comparable, with TN removal efficiencies of 87.9% and 87.0%, respectively. Both effluents contain no nitrite, with ammonium concentrations at about 14.5 mg N L^{-1} for both systems. The effluent nitrate concentrations are slightly different, which is 46.0 mg N L^{-1} in AOA-Anammox MABR while 50.5 mg N L^{-1} in AOB-Anammox MABR. The higher or comparable TN removal efficiency reveals the feasibility of the AOA-Anammox MABR for nitrogen removal under both low- and high-strength ammonium conditions.

The steady-state microbial community distribution and the resulting substrate profiles along the biofilm of both AOA-Anammox and AOB-Anammox MABR systems for low- (Scenario 1) and high-strength (Scenario 2) ammonium conditions are shown in Figure 2. Under low-strength condition, AOA are dominant in the middle (i.e., 50 – 120 μm) of the biofilm while Anammox are dominant at the outer

layer (i.e., 120 – 200 μm) of the biofilm in AOA-Anammox MABR (Figure 2A), which is due to the counter diffusion of DO from the membrane lumen and dissolved substrates from the bulk liquid. In contrast, AOB are the dominant species near the inner layer (i.e., 0 – 75 μm) of biofilm while Anammox at the outer layer (i.e., 75 – 200 μm) in AOB-Anammox MABR (Figure 2C), also with NOB occupying a small region (0 – 20 μm) close to the biofilm base. These data are coincident with corresponding substrate profiles along the biofilm (Figures 2B and 2D). DO decreases from the base to the surface of the biofilm but NH_4^+ shows an inverse trend, resulting in the abundance of AOA or AOB near the inner layer, and Anammox near the outer layer of the biofilm in either system. Notably, NH_4^+ concentration decreases to zero at ca. 50 μm of the biofilm in AOA-Anammox MABR (Figure 2B), thus leading to the migration of AOA towards the middle of the biofilm due to the availability of substrates; while both NH_4^+ and DO are available near the base of the biofilm and therefore AOB domination is found there in AOB-Anammox MABR (Figure 2D). Also, higher NO_2^- accumulation near the biofilm surface in AOB-Anammox MABR induces the coexistence of NOB.

A different microbial distribution is observed in both high-strength MABR biofilms (Figures 2E – 2H). AOA dominate the inner layer (i.e., 0 – 150 μm) of the biofilm in AOA-Anammox MABR (Figure 2E). Similarly, AOB are dominant near the base (i.e., 0 – 50 μm) of the biofilm in AOB-Anammox MABR (Figure 2G), with the coexistence of small fractions of NOB (due to higher NO_2^- accumulation) at the base of the biofilm. These again coincide with the associated substrate profiles that NH_4^+ is available near the base of both biofilms (Figures 2F and 2H). In contrast, the highest proportion of Anammox is found at around the middle of the biofilms in both systems, mainly due to unavailability of NO_2^- near the surface of the biofilm (Figures

2F and 2H). These observations clearly illustrate that the stratification of the microbial community along the biofilm depth is determined by the kinetic differences between AOA and AOB and thus their substantially different microbial interactions with Anammox in the biofilms.

It has been shown that the co-culture of AOA and Anammox is ubiquitous in various natural and engineering systems [18, 20, 40]. Our simulations results are in accordance with this fact and further demonstrate the good syntrophic metabolism between AOA and Anammox. Recent studies also show that AOA are abundant in activated sludge systems operated at prolonged solids retention times (SRT) [19]. Coincidently, the MABR can effectively retain the biomass and thus result in favourable conditions for AOA growth.

Sensitivity analyses were conducted to evaluate the model structure and to investigate the most determinant biokinetic parameters on the system performance of AOA-Anammox and AOB-Anammox MABRs in terms of TN removal using the AQUASIM built-in algorithms, with results shown in Figures S1 (under low-strength conditions) and S2 (under high-strength conditions) in the SI, respectively.

Specifically, as demonstrated in Figure S1, the TN removal efficiency of the low-strength AOA-Anammox MABR is most sensitive to Anammox- and AOA-related biokinetic parameters, i.e., the yield coefficients for Anammox (Y_{AMX}) and AOA (Y_{AOA}), which represent the decisive role of AOA and Anammox in the nitrogen removal of AOA-Anammox MABR. Similarly, the TN removal efficiency of the low-strength AOA-Anammox MABR is most dependent on AOB- and Anammox-related parameters, i.e., the yield coefficients for Anammox (Y_{AMX}) and AOB (Y_{AOB}).

Under high-strength conditions (Figure S2), the most sensitive parameters for the TN removal efficiency of AOA-Anammox MABR are the yield coefficients for AOA

(Y_{AOA}) and Anammox (Y_{AMX}), all NOB-related parameters, and the maximum growth rate of Anammox (μ_{AMX}). These parameters directly regulate the microbial community structure in the high-strength AOA-Anammox MABR biofilm, which therefore determines the system performance. For AOB-Anammox MABR, besides NOB-related parameters, its TN removal efficiency is most sensitive to the yield coefficients for AOB (Y_{AOB}) and Anammox (Y_{AMX}).

In the future application of the model, it is not practical to measure all of the numerous biokinetic parameters involved. Therefore, accurate determination of those particularly sensitive to the performance of low-strength or high-strength AOA-Anammox MABR (as discussed herein) in combination with reported values of other parameters could significantly reduce the calibration efforts while generating reliable results.

3.2 Impacts of oxygen surface loading on MABR systems

The impacts of different L_{O_2} on TN removal efficiency and active biomass fraction in the biofilms of both low-strength AOA-Anammox and AOB-Anammox MABR systems (Scenario 3, HRT = 0.5 d) are shown in Figures 3A and 3B. In both systems, Anammox is predominant at L_{O_2} of lower than 0.45 g m^{-2} d^{-1}. With L_{O_2} increasing from 0.19 to 0.45 g m^{-2} d^{-1}, the TN removal efficiencies increase from 40.9% to 86.3% in AOA-Anammox MABR and from 39.6% to 83.0% in AOB-Anammox MABR, due to higher availability of oxygen for ammonium oxidation. Further increasing L_{O_2} from 0.45 to 0.95 g m^{-2} d^{-1} in AOB-Anammox MABR leads to a quick buildup of NOB activity and thus nitrate formation increases, associated with a sharp drop of TN removal from 83.0% to 46.3% (Figure 3B), in agreement with the previous study that increasing oxygen loadings in AOB-Anammox MABR resulted in

system failure in terms of TN removal due to the inhibition on Anammox and proliferation of NOB [27]. In contrast, the TN removal in AOA-Anammox MABR increases further to a maximum value of 91.5% at L_{O_2} of 0.59 g m^{-2} d^{-1}, before a slow decline to 67.7% at L_{O_2} of 0.95 g m^{-2} d^{-1} (Figure 3A) due to an much less occurrence of NOB (thus also less competition on Anammox). Despite of better performance compared to AOB-Anammox MABR, oxygen loadings in AOA-Anammox MABR should also be controlled at an appropriate lower range, as a better syntrophic metabolism between AOA and Anammox can be achieved under oxygen-limited conditions [20].

The system performances and microbial structures of both high-strength MABR systems at different L_{O_2} (Scenario 5, HRT = 5 d) are shown in Figures 3C and 3D. Similarly, with L_{O_2} increasing from 0.19 to 0.85 g m^{-2} d^{-1}, the TN removal efficiencies in both systems show an increase from ca. 24% to 90% while AOA-Anammox MABR demonstrates a slightly better efficiency (i.e., ~5%) than that of AOB-Anammox MABR. When L_{O_2} further increases (i.e., higher than 0.85 g m^{-2} d^{-1}), the nitrification processes shift to nitrate formation in AOB-Anammox MABR with the increasing abundance of NOB, which could compete with AOB for oxygen and with Anammox for nitrite, and lead to the significant decline in TN removal, i.e., 57.9% at L_{O_2} of 1.90 g m^{-2} d^{-1} (Figure 3D). In comparison, the TN removal only slightly drops to ca. 80% at L_{O_2} of 1.19 g m^{-2} d^{-1} and then keeps relatively stable in the remaining from L_{O_2} of 1.19 to 1.90 g m^{-2} d^{-1} in AOA-Anammox MABR (Figure 3C), due to the relatively low fraction of NOB.

3.3 Impacts of ammonium surface loading on MABR systems

The impacts of ammonium surface loading (corresponding to HRT) on the TN

removal and microbial abundance along the biofilm of both low-strength AOA-Anammox and AOB-Anammox MABR systems (Scenario 4, L_{O_2} = 0.57 g m^{-2} d^{-1}) are shown in Figures 4A and 4B. With the increase of HRT from 0.25 to 0.40 d (decreasing in ammonium surface loading), the TN removal efficiencies in both systems increase to ca. 84%. Further increase in HRT from 0.40 to 0.75 d leads to the decline of the TN removal (i.e., from ca. 84% to 55%) in AOB-Anammox MABR system (Figure 4B), due to the observed increasing growth of NOB in ammonium-limiting and oxygen-sufficient condition (Figure 4B); while the TN removal in AOA-Anammox MABR system continues to increase to 91.1% at a HRT of 0.5 d (Figure 4A) due to the higher ammonium affinity of AOA than NOB at ammonium-limiting condition, which limits the growth of NOB. Afterward, the TN removal drops to 65.0% at a HRT of 0.75 d, as a result of the ammonium limitation on the growth of Anammox bacteria (Figure 4A). It should be noted that our simulations describe higher amount of AOA at lower ammonium surface loadings (i.e., higher HRTs), in agreement with the previous studies that larger abundance of AOA was observed at ammonium-limited conditions [20, 41, 42].

The dependency of the TN removal and microbial abundance in the biofilm of AOB-Anammox MABR on HRTs of 2 – 10 d under high-strength condition (Scenario 6, L_{O_2} = 0.76 g m^{-2} d^{-1}) presents a similar trend to that of low-strength condition (Figure 4B), with highest removal of 90.7% observed at a HRT of 5.5 d and increasing NOB abundance from 6 – 10 d (Figure 4D). In contrast, a different relationship as shown in Figure 3B is observed between HRT and the performance of the high-strength AOA-Anammox MABR (Scenario 6, L_{O_2} = 0.76 g m^{-2} d^{-1}). With the increase in HRTs, the TN removal reaches the maximum value of 91.0% at a HRT of 5.5 d and then plateaus over the remaining HRTs (Figure 4C). The active biomass

fractions of AOA and Anammox are both relatively stable over the course, with negligible abundance of NOB, again coincident with the repression of NOB by AOA in the AOA-Anammox MABR.

3.4 Optimal operational conditions for nitrogen removal in MABRs

Modelling results in Figures 3 and 4 show a strong dependency of the overall MABR performances on ammonium (HRT) and oxygen surface loadings, which may jointly determine the TN removal in AOA-Anammox and AOB-Anammox MABRs. Thus, the combinations of L_{O_2} and HRT on both MABR systems are explored (Figure 5). Figures 5A and 5B illustrate the TN removal of steady-state low-strength AOA-Anammox and AOB-Anammox MABR systems under various L_{O_2} and HRT conditions (Scenario 7, Table 3). The region for high-level TN removal (>80%) in AOB-Anammox MABR is limited in the narrow ridge-shape red area in terms of the variations of L_{O_2} and HRT (Figure 5B). Further increasing L_{O2} at any HRT would lead to the failure of TN removal. In contrast, the operating window for high-level TN removal (>80%) in AOA-Anammox MABR (Figure 5A) is much wider, with removal efficiency over 90% (dark red) under optimal operational conditions. In sum, AOA-Anammox MABR presents higher removal efficiency than that in AOB-Anammox MABR (e.g., the right of optimal region towards higher L_{O_2} and HRT), due to the less sensitivity of the system to L_{O_2} and HRT and better repression of NOB growth with the presence of AOA in the biofilm.

Figures 5C and 5D reveal the TN removal of steady-state high-strength AOA-Anammox and AOB-Anammox MABR systems under various L_{O_2} and HRT conditions (Scenario 8, Table 3). Similarly, a narrow ridge-shape optimal red region for high-level TN removal (>80%) in AOB-Anammox MABR is observed (Figure

5D). While the region for high-level TN removal (>80%) in AOA-Anammox MABR is much wider than that of AOB-Anammox MABR (Figure 5C), with optimal removal higher than 90% (i.e., dark red areas). Noticeably, excessive oxygen supply at a certain HRT or a prolonged HRT at a certain L_{O_2} will not affect the performance of high-strength AOA-Anammox MABR system.

Overall, in order to reach optimal operational conditions for nitrogen removal in low- or high-strength wastewater treatment, both ammonium and oxygen surface loadings must be well controlled in AOA-Anammox MABR to make TN removal efficiency locate in the red zone (>80%, Figure 5), which is easier and more reliable to reach due to its wider operating window for high-level TN removal, as compared to AOB-Anammox MABR.

4. Discussion

Autotrophic nitrogen removal in MABR through aerobic ammonium oxidation followed by Anammox has been demonstrated to be a promising technology with less energy consumption [6]. However, the major challenges in selecting the desired microbial community in autotrophic nitrogen removal system are related to the competition between Anammox and NOB for nitrite, and between AOB and NOB for oxygen [43]. Nitrate accumulation due to nitrite oxidation by NOB has become a clear symptom of undesired reactor performance, suppression of NOB growth to limit nitrate production in single-stage autotrophic nitrogen removal systems has been identified as one of the main challenges for successful implementation for wastewater treatment [11].

Since AOB have a slightly higher affinity to oxygen than NOB, AOB-Anammox MABR operated at low DO concentrations (bottom left in Figures 5B and 5D) can

benefit in out-selection of NOB and lead to better Anammox activity due to less competition of nitrite from NOB. In order to reach maximum TN removal efficiency (narrow ridge-shape red region in Figures 5B and 5D) in AOB-Anammox MABR system, appropriate well-controlled aeration is required at a certain HRT and thus is considered as the key factor affecting the reactor performance [10]. It has been reported that autotrophic nitrogen removal plants use a large number of online sensors for monitoring or control purposes [9]. Among them, the DO concentration is the most used and incorporated parameter, and failure in the DO signal can lead to severe consequences in process performance (top right in Figures 5B and 5D). Excessive oxygen supply may not be detected immediately due to DO sensor problems, which would lead to an increase in nitrate production from 10% to 40% as a result from NOB growth and Anammox inactivation [9].

In contrast, the AOA-Anammox MABR system has a much wider high-level TN removal region (wide ridge-shape red region in Figures 5A and 5C) regarding DO or HRT variations under both low- and high-strength conditions, which provide an attractive alternative to the AOB-Anammox MABR with better operating flexibility and more reliable performance responding to potential variable oxygen supply in real application. For instance, an accidental oversupply of DO would not necessarily result in an increase of NOB activity, ensuring the stability of the system performance. In addition, the system might also encounter a dynamic influent loading with highly variant ammonium. The AOA-Anammox MABR also shows better resistance to such variations. The reason is attributed to the relatively low oxygen affinity constant of AOA (K_{O2}^{AOA}, 0.128 mg/L), resulting in a higher Anammox activity and TN removal due to a lower $K_{O2}^{AOA} / K_{O2}^{NOB}$ [36].

Regarding the overall TN removal, the AOA-Anammox MABR usually shows a

~5% higher TN removal than that of the AOB-Anammox MABR, which means oxygen supply in the AOA-Anammox system could be cut off by ~5% while still achieving the same TN removal efficiency as that the AOB-Anammox system. Considering aeration in BNR plants can account for nearly half of the energy used in the plants [44], decreasing oxygen supply by ~5% could potentially lead to a substantial annual operation saving (i.e., 2 – 3%) in the entire wastewater treatment plant. Furthermore, a high-level nitrogen removal efficiency over 90% (dark red region in Figure 5A) can be achieved in the low-strength AOA-Anammox MABR system, potentially offering a great opportunity for main-stream Anammox technology to meet the strict high-standard water quality requirement in some countries, although a higher L_{O_2} would increase the energy cost, with specific trade-off being required to be considered.

It should be noted that a small amount of organic carbon might be present in the influent of real wastewater due to the incomplete pre- anaerobic digestion treatment, which might induce the heterotrophic growth and thus potentially affect the microbial community structure in AOA-Anammox MABR. However, such condition would only lead to minor heterotrophic growth and negligible impacts on TN removal efficiency [45, 46]. Nevertheless, efforts should also be dedicated to minimizing the residual organic carbon in the pre- anaerobic digestion liquor prior to its treatment in the proposed MABR, which not only benefits the bioenergy recovery purpose but also stabilizes the treatment efficiency in the AOA-Anammox MABR.

Ideally, the above goal in this study would be achieved if the model could be calibrated using experimental data. This is unfortunately not possible at present due to the lack of data. We have therefore chosen to conduct a simulation study by integrating well-established models describing various key biological processes to

assess the feasibility AOA-Anammox MABR process. We recognize that without being validated with data, the model predictions are preliminary and remain to be verified. However, we believe the preliminary results will already support our understanding in this system.

It has been suggested that AOA are more abundant than AOB in various natural environments when the concentrations of oxygen and ammonium are low [19, 40, 47, 48]. Gene sequence analysis has also revealed the presence of AOA in full-scale nitrifying bioreactors with long solids retention times (SRTs, i.e., >15 day) and low DO (ca. 0.5 mg/L) concentrations from municipal wastewater treatment plants (WWTPs) [16]. The dominance of AOA in a pilot-scale multilayer rapid infiltration system for domestic wastewater treatment [49], in activated sludge samples of two municipal WWTPs with low ammonium in the influent (ca. 10 mg-N/L) [41] and in a full-scale membrane bioreactor for simultaneous nitrogen and phosphate removal operated at low DO concentrations was further confirmed [18, 50]. Recently, the coupling of AOA and Anammox in a lab-scale sequencing batch reactor revealed the feasibility of this novel technology [20]. Application of AOA in nitrogen removal depends on identifying some effective methods or reactor types of enriching AOA. A long SRT is essential for retention of slow growing AOA biomass. Biofilm systems have been suggested for effective retention of slow growing biomass such as Anammox, due to the undefined SRT and their distinct substrate gradients. Therefore, MABR system provides a potential option to select AOA against AOB, as demonstrated in this work. Low DO and ammonium caused by diffusion in the biofilm of MABR (Figure 2) are also beneficial to selectively repress growth of AOB due to their lower oxygen and ammonium affinity compared to AOA [21]. In addition, AOA are not sensitive to temperature changes within the temperature range

from 8 to 20 ºC [21], potentially favouring the future implementation of the proposed novel AOA-Anammox MABR technology for main-stream application [12].

5. Conclusion

This work firstly assessed the system performance and the associated microbial community structure of an AOA-Anammox MABR under low- and high-strength ammonium conditions through mathematical modelling, which were compared to an AOB-Anammox MABR system under same conditions. The AOA-Anammox MABR demonstrated higher TN removal and lower oxygen supply, with much better repression of NOB and substantially wider operating window for high-level TN removal in terms of the variations of oxygen and ammonium loadings. The novel AOA-Anammox MABR provided an attractive alternative to previous AOB-Anammox MABR with better operating flexibility and more reliable performance responding to potential variable oxygen supply and highly dynamic ammonium feeding in real application.

Acknowledgements

This study was supported by the Australian Research Council (ARC) through Project DP130103147. Yiwen Liu acknowledges the support from the UTS Chancellor's Postdoctoral Research Fellowship. Bing-Jie Ni acknowledges the support of ARC Discovery Early Career Researcher Award (DE130100451) and Natural Science Foundation of China (51578391).

References

[1] M.C.M. van Loosdrecht, D. Brdjanovic, Anticipating the next century of wastewater treatment, Science 344 (2014) 1452-1453.

[2] T. Lotti, R. Kleerebezem, C. van Erp Taalman Kip, T.L.G. Hendrickx, J. Kruit, M. Hoekstra, M.C.M. van Loosdrecht, Anammox growth on pretreated municipal wastewater, Environ. Sci. Technol. 48 (2014) 7874-7880.

[3] A.O. Sliekers, K.A. Third, W. Abma, J.G. Kuenen, M.S.M. Jetten, CANON and Anammox in a gas-lift reactor, FEMS Microbiol. Lett. 218 (2003) 339-344.

[4] T.L.G. Hendrickx, Y. Wang, C. Kampman, G. Zeeman, H. Temmink, C.J.N. Buisman, Autotrophic nitrogen removal from low strength waste water at low temperature, Water Res. 46 (2012) 2187-2193.

[5] Y. Liu, B.-J. Ni, Appropriate Fe (II) Addition Significantly Enhances Anaerobic Ammonium Oxidation (Anammox) Activity through Improving the Bacterial Growth Rate, Scientific reports 5 (2015).

[6] A.O. Sliekers, N. Derwort, J.L.C. Gomez, M. Strous, J.G. Kuenen, M.S.M. Jetten, Completely autotrophic nitrogen removal over nitrite in one single reactor, Water Res. 36 (2002) 2475-2482.

[7] A. Joss, D. Salzgeber, J. Eugster, R. König, K. Rottermann, S. Burger, P. Fabijan, S. Leumann, J. Mohn, H. Siegrist, Full-scale nitrogen removal from digester liquid with partial nitritation and anammox in one SBR, Environ. Sci. Technol. 43 (2009) 5301-5306.

[8] S.E. Vlaeminck, A. Terada, B.F. Smets, D.V.d. Linden, N. Boon, W. Verstraete, M. Carballa, Nitrogen removal from digested black water by one-stage partial nitritation and anammox, Environ. Sci. Technol. 43 (2009) 5035-5041.

[9] S. Lackner, E.M. Gilbert, S.E. Vlaeminck, A. Joss, H. Horn, M.C.M. van Loosdrecht, Full-scale partial nitritation/anammox experiences–an application survey, Water Res. 55 (2014) 292-303.

[10] A. Joss, N. Derlon, C. Cyprien, S. Burger, I. Szivak, J. Traber, H. Siegrist, E. Morgenroth, Combined nitritation–anammox: advances in understanding process stability, Environ. Sci. Technol. 45 (2011) 9735-9742.

[11] J. Pérez, T. Lotti, R. Kleerebezem, C. Picioreanu, M.C.M. van Loosdrecht, Outcompeting nitrite-oxidizing bacteria in single-stage nitrogen removal in sewage treatment plants: A model-based study, Water Res. 66 (2014) 208-218.

[12] E.M. Gilbert, S. Agrawal, S.M. Karst, H. Horn, P.H. Nielsen, S. Lackner, Low temperature partial nitritation/anammox in a moving bed biofilm reactor treating low strength wastewater, Environ. Sci. Technol. 48 (2014) 8784-8792.

[13] S. Leininger, T. Urich, M. Schloter, L. Schwark, J. Qi, G.W. Nicol, J.I. Prosser, S.C. Schuster, C. Schleper, Archaea predominate among ammonia-oxidizing prokaryotes in soils, Nature 442 (2006) 806-809.

[14] C. Wuchter, B. Abbas, M.J.L. Coolen, L. Herfort, J. van Bleijswijk, P. Timmers, M. Strous, E. Teira, G.J. Herndl, J.J. Middelburg, Archaeal nitrification in the ocean, Proceedings of the National Academy of Sciences 103 (2006) 12317-12322.

[15] A. Sims, J. Horton, S. Gajaraj, S. McIntosh, R.J. Miles, R. Mueller, R. Reed, Z. Hu, Temporal and spatial distributions of ammonia-oxidizing archaea and bacteria

and their ratio as an indicator of oligotrophic conditions in natural wetlands, Water Res. 46 (2012) 4121-4129.

[16] H.-D. Park, G.F. Wells, H. Bae, C.S. Criddle, C.A. Francis, Occurrence of ammonia-oxidizing archaea in wastewater treatment plant bioreactors, Appl. Environ. Microbiol. 72 (2006) 5643-5647.

[17] C.M. Fitzgerald, P. Camejo, J.Z. Oshlag, D.R. Noguera, Ammonia-oxidizing microbial communities in reactors with efficient nitrification at low-dissolved oxygen, Water Res. 70 (2015) 38-51.

[18] E. Giraldo, P. Jjemba, Y. Liu, S. Muthukrishnan, Presence and significance of ANAMMOX spcs and Ammonia Oxidizing Archea, AOA, in Full Scale Membrane Bioreactors for Total Nitrogen Removal, Proceedings of the Water Environment Federation 2011 (2011) 510-519.

[19] J. You, A. Das, E.M. Dolan, Z. Hu, Ammonia-oxidizing archaea involved in nitrogen removal, Water Res. 43 (2009) 1801-1809.

[20] J. Yan, S. Haaijer, H.J.M. Op den Camp, L. Niftrik, D.A. Stahl, M. Könneke, D. Rush, J.S. Sinninghe Damsté, Y.Y. Hu, M.S.M. Jetten, Mimicking the oxygen minimum zones: stimulating interaction of aerobic archaeal and anaerobic bacterial ammonia oxidizers in a laboratory‐scale model system, Environ. Microbiol. 14 (2012) 3146-3158.

[21] D.A. Stahl, J.R. de la Torre, Physiology and diversity of ammonia-oxidizing archaea, Annu. Rev. Microbiol. 66 (2012) 83-101.

[22] P. Lam, M.M. Jensen, G. Lavik, D.F. McGinnis, B. Müller, C.J. Schubert, R. Amann, B. Thamdrup, M.M.M. Kuypers, Linking crenarchaeal and bacterial nitrification to anammox in the Black Sea, Proceedings of the National Academy of Sciences 104 (2007) 7104-7109.

[23] E. Syron, E. Casey, Membrane-aerated biofilms for high rate biotreatment: performance appraisal, engineering principles, scale-up, and development requirements, Environ. Sci. Technol. 42 (2008) 1833-1844.

[24] A. Terada, K. Hibiya, J. Nagai, S. Tsuneda, A. Hirata, Nitrogen removal characteristics and biofilm analysis of a membrane-aerated biofilm reactor applicable to high-strength nitrogenous wastewater treatment, J. Biosci. Bioeng. 95 (2003) 170-178.

[25] S. Lackner, A. Terada, H. Horn, M. Henze, B.F. Smets, Nitritation performance in membrane-aerated biofilm reactors differs from conventional biofilm systems, Water Res. 44 (2010) 6073-6084.

[26] C. Pellicer-Nàcher, S. Sun, S. Lackner, A. Terada, F. Schreiber, Q. Zhou, B.F. Smets, Sequential aeration of membrane-aerated biofilm reactors for high-rate autotrophic nitrogen removal: experimental demonstration, Environ. Sci. Technol. 44 (2010) 7628-7634.

[27] Z. Gong, S. Liu, F. Yang, H. Bao, K. Furukawa, Characterization of functional microbial community in a membrane-aerated biofilm reactor operated for completely autotrophic nitrogen removal, Bioresour. Technol. 99 (2008) 2749-2756.

[28] Z. Gong, F. Yang, S. Liu, H. Bao, S. Hu, K. Furukawa, Feasibility of a membrane-aerated biofilm reactor to achieve single-stage autotrophic nitrogen removal based on Anammox, Chemosphere 69 (2007) 776-784.

[29] A. Terada, S. Lackner, S. Tsuneda, B.F. Smets, Redox‐stratification controlled biofilm (ReSCoBi) for completely autotrophic nitrogen removal: The effect of co‐versus counter‐diffusion on reactor performance, Biotechnol. Bioeng. 97 (2007) 40-51.

[30] Y. Liu, Y. Zhang, B.-J. Ni, Evaluating Enhanced Sulfate Reduction and Optimized Volatile Fatty Acids (VFA) Composition in Anaerobic Reactor by Fe (III) Addition, Environ. Sci. Technol. 49 (2015) 2123-2131.

[31] Y. Liu, Y. Zhang, B.-J. Ni, Zero valent iron simultaneously enhances methane production and sulfate reduction in anaerobic granular sludge reactors, Water Res. 75 (2015) 292-300.

[32] Y. Liu, Q. Wang, Y. Zhang, B.-J. Ni, Zero valent iron significantly enhances methane production from waste activated sludge by improving biochemical methane potential rather than hydrolysis rate, Scientific reports 5 (2015).

[33] Y. Liu, L. Peng, X. Chen, B.-J. Ni, Mathematical Modeling of Nitrous Oxide Production during Denitrifying Phosphorus Removal Process, Environ. Sci. Technol. 49 (2015) 8595-8601.

[34] Q. Wang, J. Sun, C. Zhang, G.-J. Xie, X. Zhou, J. Qian, G. Yang, G. Zeng, Y. Liu, D. Wang, Polyhydroxyalkanoates in waste activated sludge enhances anaerobic methane production through improving biochemical methane potential instead of hydrolysis rate, Scientific Reports 6 (2016) 19713.

[35] B.-J. Ni, Z. Yuan, A model-based assessment of nitric oxide and nitrous oxide production in membrane-aerated autotrophic nitrogen removal biofilm systems, J. Membr. Sci. 428 (2013) 163-171.

[36] B.-J. Ni, B.F. Smets, Z. Yuan, C. Pellicer-Nàcher, Model-based evaluation of the role of Anammox on nitric oxide and nitrous oxide productions in membrane aerated biofilm reactor, J. Membr. Sci. 446 (2013) 332-340.

[37] L. Peng, X. Chen, Y. Xu, Y. Liu, S.-H. Gao, B.-J. Ni, Biodegradation of pharmaceuticals in membrane aerated biofilm reactor for autotrophic nitrogen removal: A model-based evaluation, J. Membr. Sci. 494 (2015) 39-47.

[38] P. Reichert, Aquasim 2.0-user manual, computer program for the identification and simulation of aquatic systems, Swiss Federal Institute for Environmental Science and Technology (EAWAG) (1998) 219.

[39] X. Hao, J.J. Heijnen, M.C.M. van Loosdrecht, Sensitivity analysis of a biofilm model describing a one-stage completely autotrophic nitrogen removal(CANON) process, Biotechnol. Bioeng. 77 (2002) 266-277.

[40] T.H. Erguder, N. Boon, L. Wittebolle, M. Marzorati, W. Verstraete, Environmental factors shaping the ecological niches of ammonia-oxidizing archaea, FEMS Microbiol. Rev. 33 (2009) 855-869.

[41] T. Limpiyakorn, P. Sonthiphand, C. Rongsayamanont, C. Polprasert, Abundance of amoA genes of ammonia-oxidizing archaea and bacteria in activated sludge of full-scale wastewater treatment plants, Bioresour. Technol. 102 (2011) 3694-3701.

[42] L. Ye, T. Zhang, Ammonia‐oxidizing bacteria dominates over ammonia‐oxidizing archaea in a saline nitrification reactor under low DO and high nitrogen loading, Biotechnol. Bioeng. 108 (2011) 2544-2552.

[43] M.K.H. Winkler, R. Kleerebezem, J.G. Kuenen, J. Yang, M.C.M. van Loosdrecht, Segregation of biomass in cyclic anaerobic/aerobic granular sludge allows the enrichment of anaerobic ammonium oxidizing bacteria at low temperatures, Environ. Sci. Technol. 45 (2011) 7330-7337.

[44] G. Tchobanoglous, F.L. Burton, H.D. Stensel, Metcalf, Eddy, Wastewater Engineering: Treatment and Reuse, McGraw-Hill Education2003.

[45] M.S.I. Mozumder, C. Picioreanu, M.C.M. van Loosdrecht, E.I.P. Volcke, Effect of heterotrophic growth on autotrophic nitrogen removal in a granular sludge reactor, Environ. Technol. 35 (2014) 1027-1037.

[46] X. Chen, J. Guo, G.-J. Xie, Y. Liu, Z. Yuan, B.-J. Ni, A new approach to simultaneous ammonium and dissolved methane removal from anaerobic digestion liquor: A model-based investigation of feasibility, Water Res. 85 (2015) 295-303.

[47] M. Labrenz, E. Sintes, F. Toetzke, A. Zumsteg, G.J. Herndl, M. Seidler, K. Jürgens, Relevance of a crenarchaeotal subcluster related to Candidatus Nitrosopumilus maritimus to ammonia oxidation in the suboxic zone of the central Baltic Sea, The ISME journal 4 (2010) 1496-1508.

[48] C.A. Francis, K.J. Roberts, J.M. Beman, A.E. Santoro, B.B. Oakley, Ubiquity and diversity of ammonia-oxidizing archaea in water columns and sediments of the ocean, Proc. Natl. Acad. Sci. U.S.A. 102 (2005) 14683-14688.

[49] Y. Lian, M. Xu, Y. Zhong, Y. Yang, F. Chen, J. Guo, Ammonia Oxidizers in a Pilot-Scale Multilayer Rapid Infiltration System for Domestic Wastewater Treatment, PloS one 9 (2014) e114723.

[50] E. Giraldo, P. Jjemba, Y. Liu, S. Muthukrishnan, Ammonia Oxidizing Archaea, AOA, Population and Kinetic Changes in a Full Scale Simultaneous Nitrogen and Phosphorous Removal MBR, Proceedings of the Water Environment Federation 2011 (2011) 3156-3168.

Table captions

Table 1. Process kinetic rate equations for the AOA-Anammox system

Table 2. Stoichiometric matrix for the AOA-Anammox system

Table 3. An overview of the scenarios for the model-based assessments

Table 1. Process kinetic rate equations for the AOA-Anammox system

Process	Kinetics rates expressions
Ammonium oxidizing archaea (AOA)	
1. Growth of AOA	$\mu_{AOA}\frac{S_{O2}}{K_{O2}^{AOA}+S_{O2}}\frac{S_{NH4}}{K_{NH4}^{AOA}+S_{NH4}}X_{AOA}$
2. Decay of AOB	$b_{AOA}X_{AOA}$
Nitrite oxidizing bacteria (NOB)	
3. Growth of NOB	$\mu_{NOB}\frac{S_{O2}}{K_{O2}^{NOB}+S_{O2}}\frac{S_{NO2}}{K_{NO2}^{NOB}+S_{NO2}}X_{NOB}$
4. Decay of NOB	$b_{NOB}X_{NOB}$
Anaerobic ammonium oxidizing bacteria (Anammox)	
5. Growth of anammox	$\mu_{AMX}\frac{K_{O2}^{AMX}}{K_{O2}^{AMX}+S_{O2}}\frac{S_{NH4}}{K_{NH4}^{AMX}+S_{NH4}}\frac{S_{NO2}}{K_{NO2}^{AMX}+S_{NO2}}X_{AMX}$
6. Decay of anammox	$b_{AMX}X_{AMX}$
Heterotrophic bacteria (HB)	
7. Hydrolysis	$k_H\frac{X_S/X_H}{K_X+X_S/X_H}X_H$
8. Aerobic growth of HB	$\mu_H\frac{S_{O2}}{K_{OH1}+S_{O2}}\frac{S_S}{K_{S1}+S_S}X_H$
9. Anoxic growth of HB with nitrate reduction	$\mu_H\eta_{H1}\frac{K_{OH2}}{K_{OH2}+S_{O2}}\frac{S_{NO3}}{K_{NO3}^{HB}+S_S}\frac{S_S}{K_{S2}+S_S}X_H$
10. Anoxic growth of HB with nitrite reduction	$\mu_H\eta_{H2}\frac{K_{OH3}}{K_{OH3}+S_{O2}}\frac{S_{NO2}}{K_{NO2}^{HB}+S_{NO2}}\frac{S_S}{K_{S3}+S_S}X_H$
11. Decay of HB	$b_H X_H$

Table 2. Stoichiometric matrix for the AOA-Anammox system

Variable	S_{O2}	S_S	S_{NH4}	S_{NO2}	S_{NO3}	S_{N2}	X_S	X_H	X_{AOA}	X_{NOB}	X_{AMX}	X_I
Process	O_2	COD	N	N	N	N	COD	COD	COD	COD	COD	COD
1	$-\frac{3.43-Y_{AOA}}{Y_{AOA}}$		$-i_{NBM}-\frac{1}{Y_{AOA}}$	$\frac{1}{Y_{AOA}}$					1			
2			$i_{NBM}-i_{NXI}f_I$				$1-f_I$		-1			f_I
3	$-\frac{1.14-Y_{NOB}}{Y_{NOB}}$		$-i_{NBM}$	$-\frac{1}{Y_{NOB}}$	$\frac{1}{Y_{NOB}}$					1		
4			$i_{NBM}-i_{NXI}f_I$				$1-f_I$			-1		f_I
5			$-i_{NBM}-\frac{1}{Y_{AMX}}$	$-\frac{1}{Y_{AMX}}-\frac{1}{1.14}$	$\frac{1}{1.14}$	$\frac{2}{Y_{AMX}}$					1	
6			$i_{NBM}-i_{NXI}f_I$				$1-f_I$				-1	f_I
7		1	i_{NXS}				-1					
8	$-\frac{1-Y_H}{Y_H}$	$-\frac{1}{Y_H}$	$-i_{NBM}$					1				
9		$-\frac{1}{Y_H}$	$-i_{NBM}$		$-\frac{1-Y_H}{2.86Y_H}$	$\frac{1-Y_H}{2.86Y_H}$		1				
10		$-\frac{1}{Y_H}$	$-i_{NBM}$	$-\frac{1-Y_H}{1.71Y_H}$		$\frac{1-Y_H}{1.71Y_H}$		1				
11			$i_{NBM}-i_{NXI}f_I$				$1-f_I$	-1				f_I

Table 3. An overview of the scenarios for the model-based assessments

Scenarios	Simulation conditions	Variable conditions
Scenario 1 Standard simulation of the partial nitritation (AOA or AOB) -Anammox biofilm system under low-strength condition	S_{NH4} = 30 mg N L^{-1} HRT = 0.5 d L_{O2} = 0.45 g m^{-2} d^{-1} L_f = 200 µm	
Scenario 2 Standard simulation of the partial nitritation (AOA or AOB) -Anammox biofilm system under high-strength condition	S_{NH4} = 500 mg N L^{-1} HRT = 5 d L_{O2} = 0.95 g m^{-2} d^{-1} L_f = 500 µm	
Scenario 3 Effect of L_{O2} on the partial nitritation (AOA or AOB) -Anammox biofilm system under low-strength condition	S_{NH4} = 30 mg N L^{-1} HRT = 0.5 d L_f = 200 µm	L_{O2} = 0.19 – 0.95 g m^{-2} d^{-1}
Scenario 4 Effect of HRT on the partial nitritation (AOA or AOB) -Anammox biofilm system under low-strength condition	S_{NH4} = 30 mg N L^{-1} L_{O2} = 0.57 g m^{-2} d^{-1} L_f = 200 µm	HRT = 0.25 – 0.75 d
Scenario 5 Effect of L_{O2} on the partial nitritation (AOA or AOB) -Anammox biofilm system under high-strength condition	S_{NH4} = 500 mg N L^{-1} HRT = 5 d L_f = 500 µm	L_{O2} = 0.19 – 1.90 g m^{-2} d^{-1}
Scenario 6 Effect of HRT on the partial nitritation (AOA or AOB) -Anammox biofilm system under high-strength condition	S_{NH4} = 500 mg N L^{-1} L_{O2} = 0.76 g m^{-2} d^{-1} L_f = 500 µm	HRT = 2 – 10 d
Scenario 7 Combined effects of HRT and L_{O2} on the partial nitritation (AOA or AOB) -Anammox biofilm system under low-strength condition	S_{NH4} = 30 mg N L^{-1} L_f = 200 µm	HRT = 0.25 – 0.75 d L_{O2} = 0.19 – 0.95 g m^{-2} d^{-1}
Scenario 8 Combined effects of HRT and L_{O2} on the partial nitritation (AOA or AOB) -Anammox biofilm system under high-strength condition	S_{NH4} = 500 mg N L^{-1} L_f = 500 µm	HRT = 2 – 10 d L_{O2} = 0.19 – 1.90 g m^{-2} d^{-1}

Figure captions

Figure 1. Simplified representation of the key biochemical processes associated with the microorganisms involved in the two biofilm systems: (A) AOA-Anammox MABR; and (B) AOB-Anammox MABR.

Figure 2. Modelling results of microbial and substrate profiles along the depth of the two MABR biofilms (depth zero represents the membrane surface, i.e., the base of the biofilm) under both low- and high-strength ammonium conditions: (A-B) microbial population distribution and substrate profiles in low-strength AOA-Anammox MABR; (C-D) microbial population distribution and substrate profiles in low-strength AOB-Anammox MABR; (E-F) microbial population distribution and substrate profiles in high-strength AOA-Anammox MABR; and (G-H) microbial population distribution and substrate profiles in high-strength AOB-Anammox MABR.

Figure 3. Modelling results of the impacts of oxygen surface loading (L_{O_2}) on the system performance and microbial abundance under both low- and high-strength ammonium conditions: (A) low-strength AOA-Anammox MABR; (B) low-strength AOB-Anammox MABR; (C) high-strength AOA-Anammox MABR; and (D) high-strength AOB-Anammox MABR.

Figure 4. Modelling results of the impacts of ammonium surface loading (or HRT) on the system performance and microbial abundance under both low- and high-strength ammonium conditions: (A) low-strength AOA-Anammox MABR; (B) low-strength AOB-Anammox MABR; (C) high-strength AOA-Anammox MABR; and (D) high-strength AOB-Anammox MABR.

Figure 5. Modelling results of the dependency of the TN removal on the simultaneous variations of oxygen surface loading (L_{O_2}) and HRT under both low- and high-strength ammonium conditions: (A) low-strength AOA-Anammox MABR; (B) low-strength AOB-Anammox MABR; (C) high-strength AOA-Anammox MABR; and (D) high-strength AOB-Anammox MABR. The color scale represents the TN removal efficiency in %.

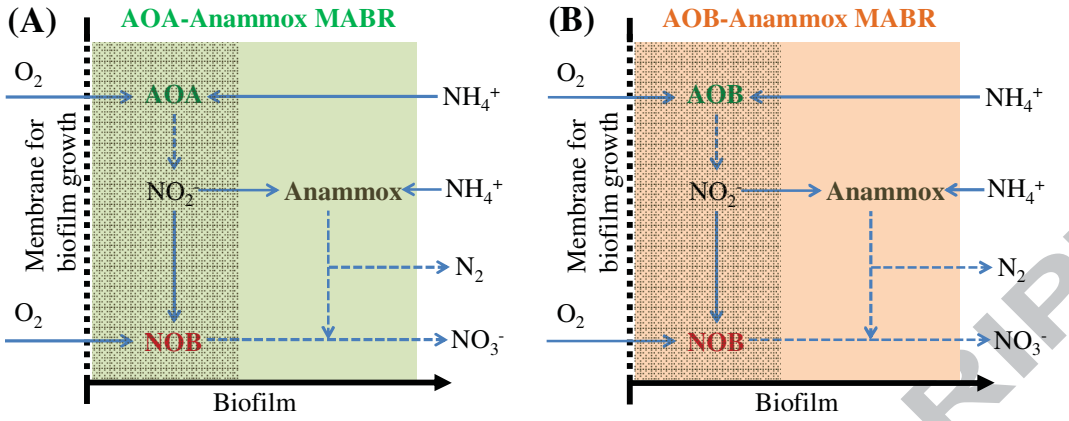

Figure 1. Simplified representation of the key biochemical processes associated with the microorganisms involved in the two biofilm systems: (A) AOA-Anammox MABR; and (B) AOB-Anammox MABR.

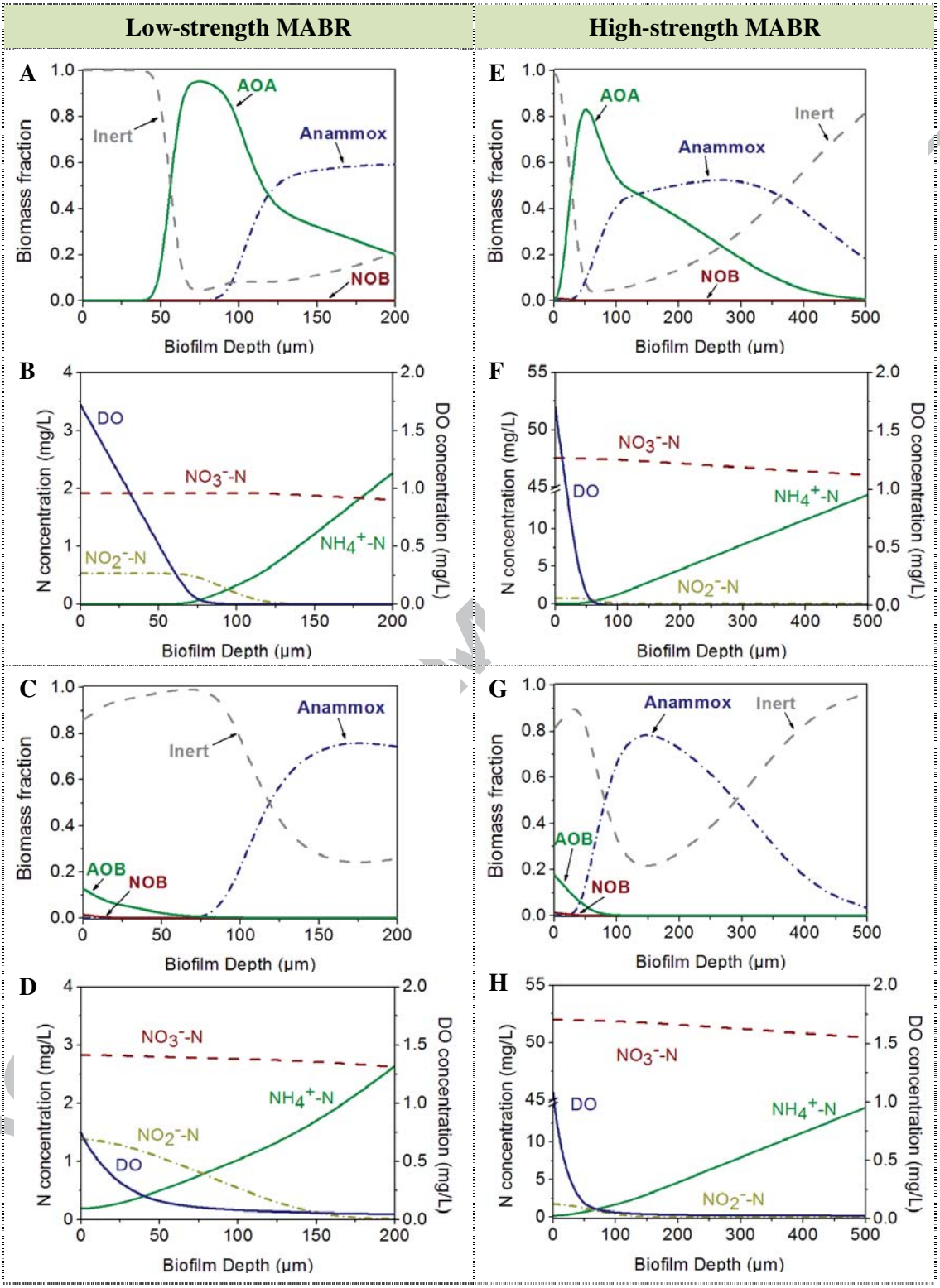

Figure 2. Modelling results of microbial and substrate profiles along the depth of the two MABR biofilms (depth zero represents the membrane surface, i.e., the base of the

biofilm) under both low- and high-strength ammonium conditions: (A-B) microbial population distribution and substrate profiles in low-strength AOA-Anammox MABR; (C-D) microbial population distribution and substrate profiles in low-strength AOB-Anammox MABR; (E-F) microbial population distribution and substrate profiles in high-strength AOA-Anammox MABR; and (G-H) microbial population distribution and substrate profiles in high-strength AOB-Anammox MABR.

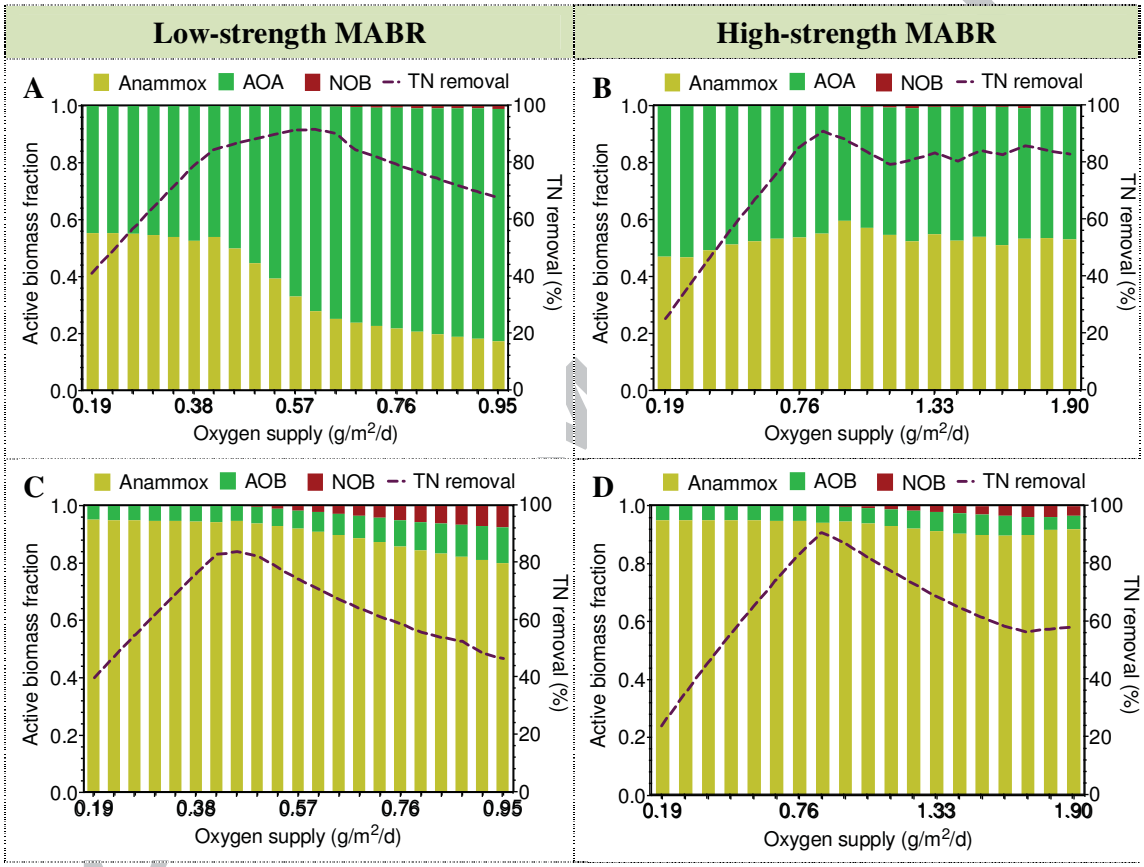

Figure 3. Modelling results of the impacts of oxygen surface loading (L_{O_2}) on the system performance and microbial abundance under both low- and high-strength ammonium conditions: (A) low-strength AOA-Anammox MABR; (B) low-strength AOB-Anammox MABR; (C) high-strength AOA-Anammox MABR; and (D) high-strength AOB-Anammox MABR.

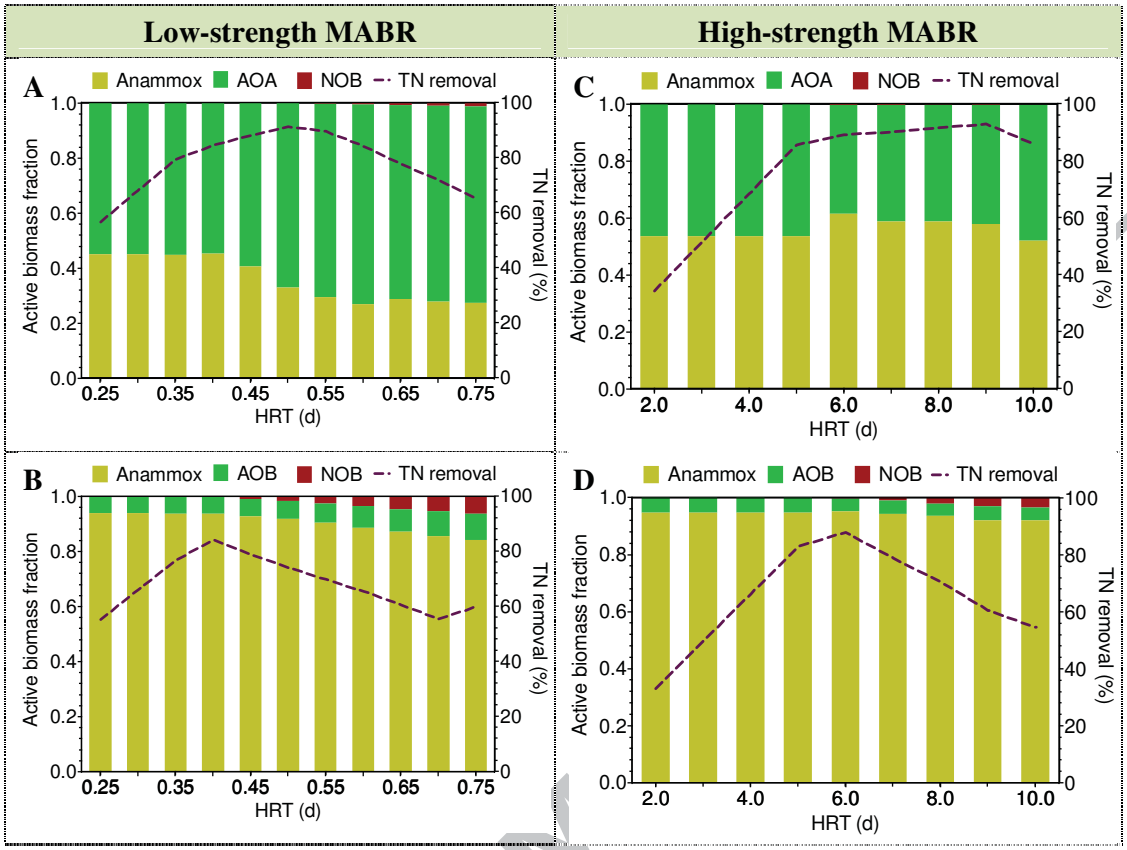

Figure 4. Modelling results of the impacts of ammonium surface loading (or HRT) on the system performance and microbial abundance under both low- and high-strength ammonium conditions: (A) low-strength AOA-Anammox MABR; (B) low-strength AOB-Anammox MABR; (C) high-strength AOA-Anammox MABR; and (D) high-strength AOB-Anammox MABR.

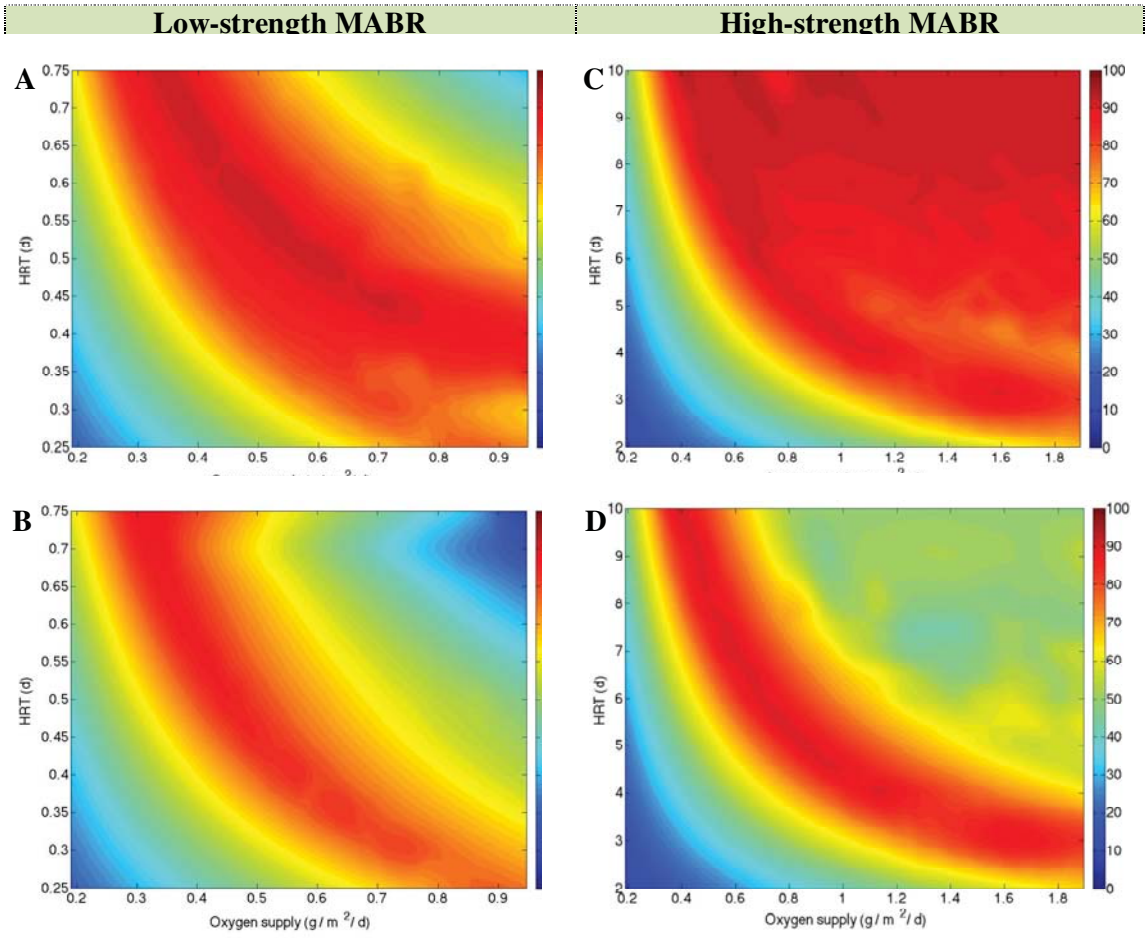

Figure 5. Modelling results of the dependency of the TN removal on the simultaneous variations of oxygen surface loading (L_{O_2}) and HRT under both low- and high-strength ammonium conditions: (A) low-strength AOA-Anammox MABR; (B) low-strength AOB-Anammox MABR; (C) high-strength AOA-Anammox MABR; and (D) high-strength AOB-Anammox MABR. The color scale represents the TN removal efficiency in %.

Highlights

- System performance of AOA-Anammox MABR was assessed using mathematical modeling
- AOA-Anammox MABR shows higher TN removal/lower oxygen supply than AOB-Anammox MABR
- AOA-Anammox MABR shows wider operating window for high-level TN removal
- This study provides first insight on design and operation of novel AOA-Anammox MABR

Graphic abstract